Research on Carrier Mobility of few-layer MoO_3

Qian Qu

Guangdong University of Science & Technology, Dongguan 523083, China.

Abstract

New two-dimensional semiconductors with high carrier mobility and excellent stability are the basis for the development of next-generation high-speed and low-power nanoelectronic devices. Due to its abundant reserves, inherent band gap and stable chemical properties, metal oxides have recently been suggested as potential electronic materials. However, their carrier mobility is usually on the order of tens of square centimeters per volt per second, which is much lower than that of commonly used silicon. Through first-principles calculations and deformation potential theory, we predict that the few-layer MoO3 is a chemically stable wide band gap semiconductor, and the acoustic phonon carrier mobility of electrons and holes is greater than 3000 cm2V-1s-1. This makes few layers of MoO3 promising for future electron and hole transport applications. In addition, we also found that the carrier mobility has a large anisotropy in the plane, and its ratio reaches about 20-30 times. The combined effect of elastic modulus and deformation potential anisotropy makes the few-layer MoO3 not only have high mobility, but also exhibit strong transmission anisotropy. This indicates that the few layers of MoO3 are a promising candidate material for electron and hole transport applications. In addition, we also suggest that by reasonably controlling the direction of carrier transfer, the performance of the device can be greatly promoted.

Keywords

Electronic devices, carrier mobility, few layers of MoO3, anisotropy.

1. Introduction

Due to the remarkable electrical, mechanical and optical properties of two-dimensional (2D) crystals, materials science has been revolutionized. In the past few years, a large number of new 2D materials such as graphene, MoS2 and black phosphorus have been discovered, and it is suggested that they are promising candidates for future electronic devices. It is well known that graphene has a very high electron mobility (~105cm2V-1s-1) [1], but natural graphene lacks an inherent band gap, which limits its practical application in field effect transistors (FET). Unlike graphene, transition metal sulfides (TMDCs) have a large inherent band gap. For example, MoS2 is considered an important substitute material for graphene [2,3], and its on/off ratio is as high as 1×108, extremely low Standby power consumption has been realized in a series of MoS2. However, the carrier mobility of typical TMDC devices is still lower than 300cm2V-1s-1, which is not competitive with commonly used silicon. Recently, a few layers of phosphene have been successfully stripped, and its band gap increased from 0.35 to 1.51eV with the thickness [4]. At the same time, it was found that the carrier mobility of phosphorene-based FET is as high as 1000cm2V-1s-1, and the on/off ratio is as high as 104-105, and other two-dimensional phosphorus isotopes and derived one-dimensional (1D) nanostructures have also been found to have ultra-high carrier mobility. However, these phosphorus-based 2D materials are unstable in air and will be rapidly degraded under environmental conditions. Although many efforts have been made, the performance of phosphorus-based 2D material FETs has not exceeded that of general silicon-based devices. Therefore, it is inevitable to explore new 2D semiconductor materials with higher carrier mobility and excellent stability.

Layered transition metal oxide is a material with excellent stability and has been used in many industries. Among them, layered molybdenum trioxide (MoO3) with a high relative permittivity has been widely used, such as gas sensors[5], photochromic and electrochromic devices[6], storage materials[7] and catalysts[8]. MoO3 has very weak interlayer van der Waals (vdW) force, which can

peel stable single-layer nanosheets from the bulk. At the same time, few-layer MoO3 nanosheets can be synthesized by mechanical peeling, liquid exfoliation and intercalation, epitaxial growth, and oxidation of MoS2 nanosheets. On the other hand, although metal oxides are suggested as candidate materials for electronic and optoelectronic materials due to their natural abundance and good stability, their carrier mobility is usually on the order of tens of square centimeters per volt per second. This is too low for actual electronic equipment. Recently, Balendhran et al.[9] peeled off the few layers of MoO3 nanosheets from α-MoO3 and reduced them to MoO3-x below the stoichiometry, and found that the carrier mobility of the fabricated 2D FET exceeded 1100cm2V-1s-1. In addition, Alsaif et al.[10] used sunlight to induce the generation of oxygen vacancies in an aqueous environment, which improved the electronic properties of 2D MoO3-x stripped from the liquid phase, and the carrier mobility in the fabricated device reached 600 cm2V-1s-1, and the free electron concentration is 1.6×1021 cm-3, the current on/off ratio is greater than 105, improved overall performance.

Obviously, the carrier mobility observed in MoO3 flakes is higher than 1000 cm2V-1s-1, which is about an order of magnitude higher than that of typical oxides. Therefore, it is important to explain the underlying mechanism of this high mobility. Like most metal oxides, MoO3 has a wide band gap (~3.0eV) in its stoichiometric form, resulting in a lower carrier concentration, which is not suitable for electronic devices. However, MoO3 can be reduced to substoichiometric MoO3-x through ion intercalation processes (such as hydrogen ions and sunlight), so that the energy gap can be reasonably adjusted by controlling the oxygen vacancy. In low-k materials, the introduction of vacancies will increase the number of Coulomb charges, which will dominate electron scattering, but MoO3 is a high-k material, and its high relative permittivity (> 500) can minimize Coulomb scattering. It was found that acoustic phonon scattering has the greatest impact at room temperature[9]. Therefore, only considering the carrier mobility of acoustic phonon scattering should represent the theoretical limit of MoO3 carrier transmission. As the most basic step, it is very important to understand the carrier mobility of the original few-layer MoO3.

In the current work, we have studied the carrier mobility confined by the acoustic phonons of few layers of MoO3 through first-principles calculations and deformation potential theory. The optB88-vdW and HSE06 functionals were used to deal with the vdW interaction between layers and calculate the energy gap accurately. Our calculations show that the few-layer MoO3 system is a chemically stable wide band gap semiconductor. Their carrier mobility at room temperature is predicted to be very high, up to 3000 cm2V-1s-1, and they also exhibit strong anisotropic behavior. It is found that the higher mobility of the predicted low-layer MoO3 and its transmission anisotropic behavior depend on the combined effect of the direction-dependent elastic modulus and the deformation potential.

2. Calculation method

Since the coherent wavelength of thermally activated carriers in inorganic semiconductors such as MoO3 at 300K is usually close to the coherent wavelength of the acoustic phonon mode in the center of the Brillouin zone, acoustic phonon scattering will dominate the carrier transmission in the low-energy region. Because optical-phonon scattering[11] is mainly important for high-energy carriers, it is not considered in this work. For example, the electron-acoustic-phonon coupling proposed by Bardeen and Shockley[12] can be effectively calculated by deformation potential theory, and has been widely used to study the carrier mobility of different 2D materials. According to the effective mass approximation, the acoustic-phonon-limited carrier mobility is given by:

$$\mu_{2D} = \frac{e\hbar^3 C_{2D}}{k_B T m m_d (E_1^i)^2} \tag{1}$$

The effective carrier mass (effective transmission mass) mx/y* in the transmission direction is expressed as $\hbar^2\left[\frac{\partial^2 E(k)}{\partial k^2}\right]^{-1}$. The average effective mass (effective density of states (DOS) mass) md

is defined as $\sqrt{m_x^* m_y^*}$. E1i represents the deformation potential of the maximum value of the valence band (VBM) of a hole or the minimum value of the conduction band (CBM) of an electron along the transport direction, which is defined as $\frac{\Delta V}{\Delta l/l_0}$. Here l_0 is the lattice constant in the transmission direction, and Δl is the deformation compared to l_0, and ΔV is the change in the band edge of CBM and VBM under uniaxial strain. The elastic modulus C2D in the x and y directions is defined as $(E-E_0)/S_0 = C(\Delta l/l_0)^2/2$, where E is the total energy and S0 is the area of the 2D balanced structure. All calculated data use a 0.5% strain step. A temperature of 300k is used in the mobility calculation. It has been proved that the calculation method of carrier mobility is not only computationally effective, but also physically reasonable. There are other more complex methods, such as the Boltzmann transmission method with approximately available relaxation times, which can more accurately describe the carrier mobility.

All density functional theory (DFT) calculations use the Vienna ab initio simulation software package code, and are performed in the affixed projected plane wave and generalized gradient approximation. Because the Perdew-Burke-Ernzerhof (PBE) functional cannot reasonably describe the inter-layer vdW force, the optB88-vdW functional[13] is used in the calculation of the few-layer MoO3 in this paper. In addition, it is known that the energy gap is mainly underestimated in the (semi-)localized functional, so the HSE06 calculation is used to obtain the physical properties related to the energy band structure, including effective mass and deformation potential. Our previous research proved that this combination can give a relatively reasonable description of layered semiconductors. Therefore, the elastic modulus obtained by the optB88-vdW functional and the effective mass and deformation potential obtained by the HSE06 functional are used to estimate the carrier mobility of the few layers of MoO3, and the results obtained by the optB88-vdW functional are also listed for use Compare. Because there is no expected vdW interaction in the single-layer MoO3, the PBE method is used for calculation. In order to avoid layer-to-layer interaction in the few-layer MoO3 supercell, we added a vacuum layer of at least 15 Å. The cut-off energy is set to 650eV for plane wave basis set calculation, and the Monkhorst-Pack k-point is 10×9×1. In the calculation, only the atomic coordinates are optimized, and the accuracy is that the maximum stress on each atom is not greater than 2×10-2eV Å-1. When using HSE06 calculation, in order to increase the calculation rate, the cutoff can be reduced to 450 eV to reduce the amount of calculation.

3. Results and discussion

A few layers of MoO3 are cut from the block layered α-MoO3 structure for the calculations in this paper. The MoO6 octahedrons shared by the edges form a twisted two-layer structure and are arranged in an aba manner. The two layers of the two-layer and three-layer MoO3 are stacked in ab and aba ways, the same as in the block. As shown in Figure 1, the single-layer MoO3 sheet is a rectangular unit cell with lattice constants x(a) and y(b) of 3.721 Å and 3.919 Å, respectively. Compared with the values, they are all a bit smaller, and their values are 3.738 Å and 3.942 Å, respectively. The corresponding lattice constants calculated using PBE functionals are 3.708Å and 3.955Å, respectively. The unit cell of a single layer of MoO3 is composed of a twisted edge sharing MoO6 octahedron, in which there are three unique O atoms marked with different colors. As shown in the figure 1, the top Oa atoms that are single-coordinated to Mo atoms are arranged along the z(c) direction, while the three-edge shared Oe atoms are arranged on the x(a) axis and are three-coordinated to Mo atoms. In the y(b) direction, we can find that the corners share the asymmetric double coordination of Oc and Mo atoms. The lattice constants a and b of double-layer and triple-layer MoO3 predicted by the optB88-vdW functional are 3.729 Å and 3.933 Å, and 3.731 Å and 3.930 Å, respectively. We define the difference in z-coordinates of two adjacent Mo atoms between different double-layers as the inter-layer distance, which is about 4.044Å for the double-layer system. For the three-layer MoO3, the spacing between the two layers is symmetrical and both equal to 4.039Å.

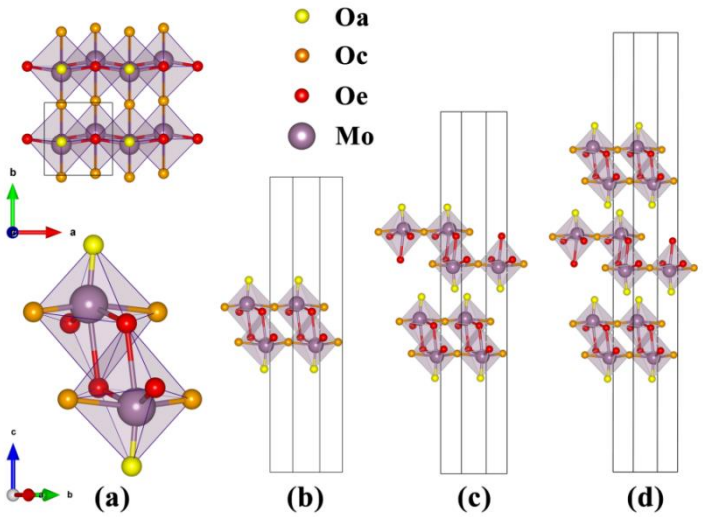

Fig. 1 The crystal structure of few layers of MoO3. (a) The top view of a single layer of MoO3 (top) and the edges share the details of the MoO6 octahedral unit (bottom). (b-d) Single-layer, double-layer and triple-layer MoO3 (1×2) crystal units.

We calculated the energy band structure of the few-layer MoO3 system using two functionals, optB88-vdW and HSE06, as shown in Figure 2. We can find that the few-layer MoO3 predicted by the two methods are indirect semiconductors, with VBM at S (0.5, 0.5) and CBM at Γ (0, 0). The band gaps of single-layer, double-layer and triple-layer MoO3 obtained by the optB88-vdW method are 1.796, 1.750 and 1.745 eV, and the corresponding bulk band gap is 1.673 eV. In addition to the larger energy gap, the HSE06 calculation gives a very similar energy distribution, with values of 2.896, 2.873 and 2.861 eV for one to three levels, respectively. In order to further understand the underlying mechanism, we give a detailed atomic and atomic orbital projection DOS in Figure 3. As shown in the figure 3, the O 2p orbital dominates the electronic state near the VBM and overlaps the Mo 4d state in the energy range of -6 to -2 eV, while the density of states near the CBM is mainly composed of the Mo 4d orbital and slightly mixed in the O 2p state. Further analysis shows that the O 2p orbital of VBM is mainly composed of the py orbital of Oe atom and the px orbital of Oc atom. The electronic state of CBM is mainly composed of in-plane Mo dxy orbitals, accompanied by weak hybridization of Oc and Oa atoms px orbitals. At the same time, the space charge density distribution of VBM and CBM are given. As shown in Figure 2(g), in the case of VBM, the py and px orbital charge density distributions can be seen around Oe and Oc atoms. For CBM, the charge density of Mo atoms is usually dxy orbitals. At the same time, it was also found that the px orbitals are located around Oc and Oa atoms.

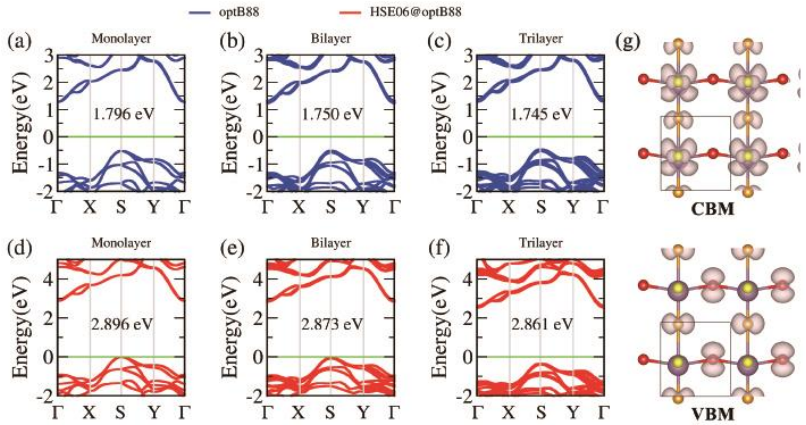

Fig. 2 Energy band structure of few layers of MoO3 calculated using optB88-vdW and HSE06 functional.The energy bands of single-layer, double-layer and triple-layer MoO3 calculated using optB88-vdW are given in parts a-c, respectively. The corresponding HSE06 results are given in

section d-f. The charge density of the VBM (bottom) and CBM (top) of a single layer of MoO3 is given in g, where the isosurface is set to 0.01 e born-3. Since the charge density is symmetric between the top and bottom in the double-layer MoO3 structure, only the charge density at the top of the structure is given.

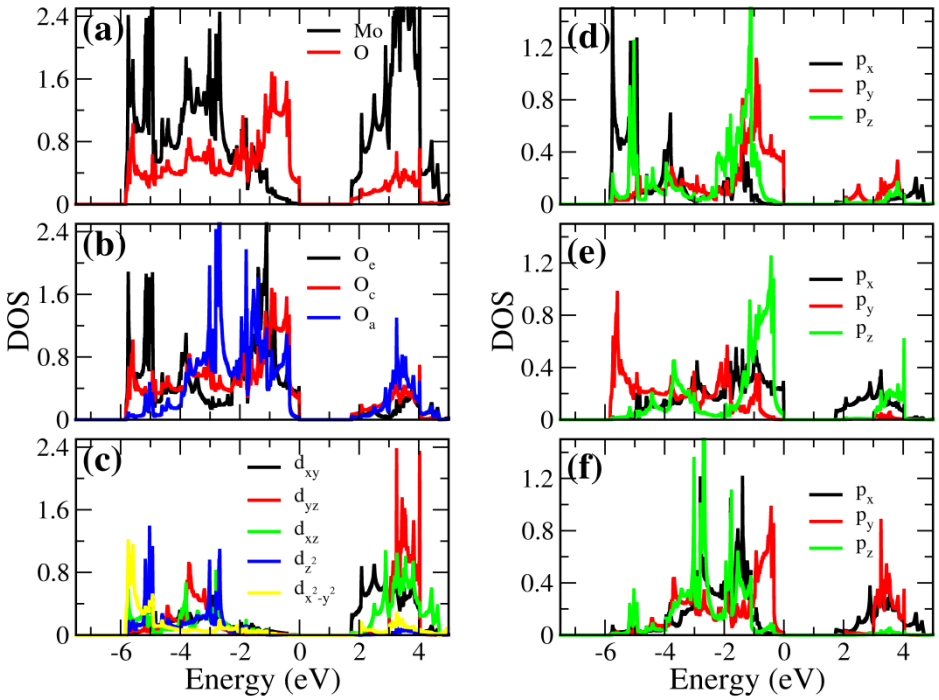

Fig. 3 The projected DOS of a single-layer MoO3 calculated using optB88-vdW. The HSE06 functional gives similar results except for a larger band gap. The partial DOS of Mo 4d and O 2p orbitals is shown in Figure a. Figure b shows the projected DOS of three different O atoms. Figure (c-f) shows the projected DOS of Mo, Oe, Oc and Oa atomic orbitals.

As shown in Equation 1, the acoustic phonon-limited carrier mobility of 2D materials can be predicted based on the elastic modulus, effective mass, and deformation potential constant. Therefore, we first discussed the modulus of elasticity of the few layers of MoO3. For single-layer MoO3, we used the PBE method to calculate the elastic modulus in the x and y directions of the 2D plane, and the values were 141.16 and 85.06 Jm-2, respectively. At the same time, the results obtained by using the optB88-vdW functional correspond to 152.80 and 95.64 Jm-2. These values are greater than black phosphorus[4] (28.94-101.60 Jm-2) and MoS2[14] (127.44 Jm-2), but are about 2 to 3 times smaller than those of graphene[15]. However, we found that the in-plane two-dimensional elastic modulus exhibits very interesting anisotropy, and the reason for the strong anisotropy is the focus of later research.

Because the PBE functional failed to describe the vdW interaction, we used the optB88 method to discuss the results of two-layer and three-layer MoO3. It can be seen from the data in Table 1 that the 2D elastic modulus in the x and y directions has increased from 332.19 and 205.09 Jm-2 of double-layer MoO3 to 516.14 and 317.09 Jm-2 of three-layer MoO3. The obvious in-plane anisotropic behavior of elastic modulus is still maintained in the few-layer system. At the same time, we also found that there is a strong interlayer coupling between the two layers in the few-layer MoO3 structure. If the interlayer coupling between the double layers in the few layers of MoO3 is weak, the elastic modulus of the double and triple layers of MoO3 will be 2 and 3 times that of the single layer. However, we found that the elastic modulus of the double-layer and triple-layer MoO3 in the x and y directions is 2.17 and 2.14 times, and 3.38 and 3.31 times that of the single layer. This indicates that the elastic coupling between the two layers increases with the thickness in the few-layer system. This strong coupling between double layers can also be understood by the fact that the distance between two adjacent vertices Oa atoms in different double layers is very short. For the two-layer and three-layer MoO3, the O-O distances are 2.773 and 2.776 Å, respectively, which exhibit mutual

repulsion during compression, which results in a strong coupling of the elastic modulus between the layers.

Table 1 Predicted electron and hole deformation potential (E1), 2D elastic modulus (C2D), effective mass (m*) and mobility of the few layers of MoO3 in the x and y directions under a 300K environment.

type	layer	m_x^*/m_0	m_y^*/m_0	E_1^x/eV	E_1^y/eV	C_x^{2D}/Jm^{-2}	C_y^{2D}/Jm^{-2}	μ_x/cm^{2}V^{-1}s^{-1}	μ_y/cm^2 V^{-1} s^{-1}
					PBE				
e	1	0.873	0.594	1.724	10.628	141.16	85.06	1608.81	37.52
h	1	2.064	0.974	1.133	7.166	141.16	85.06	800.57	25.56
					optB88				
e	1	0.993	0.641	1.907	10.956	152.80	95.64	1130.02	33.18
	2	0.949	0.615	2.085	10.842	332.19	205.09	2245.89	79.12
	3	0.953	0.616	2.257	10.774	516.14	317.09	2953.39	123.18
h	1	2.291	0.966	1.470	7.2392	152.80	95.64	441.81	27.03
	2	1.853	0.963	1.120	6.307	332.19	205.09	2277.43	85.34
	3	1.918	0.949	0.916	6.293	516.14	317.09	5066.16	133.31
					HSE06				
e	1	1.056	0.588	2.220	11.443	152.80	95.64	793.59	33.60
	2	0.927	0.563	2.621	11.944	332.19	205.09	1538.80	75.26
	3	0.972	0.562	2.112	12.417	516.14	317.09	3430.51	105.50
h	1	1.669	0.910	1.999	9.538	152.80	95.64	396.35	19.99
	2	1.557	0.900	1.351	7.187	332.19	205.09	2101.91	79.42
	3	1.578	0.901	1.499	7.543	516.14	317.09	2600.11	110.54

Now, we turn our attention to the effective mass of carriers. As shown in Figure 4 and 5, using optB88-vdW and HSE06 to calculate the effective mass of the few layers of MoO3, the energy distribution is parabolic around the VBM and CBM, showing typical free electron characteristics. Through quadratic fitting, we can get the effective mass of electrons and holes in the x and y directions. It is found from Table 1 that the effective mass of carriers in the y direction is usually smaller than the x direction, and the effective mass of electrons is always smaller than the effective mass of holes. The electron effective masses of the few layers of MoO3 calculated by the HSE06 functional are 1.056 and 0.588, 0.927 and 0.563, 0.972 and 0.562m0 in the x and y directions, respectively, which are all larger than MoS2[14] (0.48m0), and have certain competitiveness. The effective mass of the hole is 1.557-1.669 and 0.90-0.91m0 in the x and y directions, respectively. It can be seen that the result of optB88-vdW is closer to the result of HSE06, while the PBE functional gives a slightly smaller effective mass. All the effective masses of electrons and holes predicted by functionals show strong directional anisotropy.

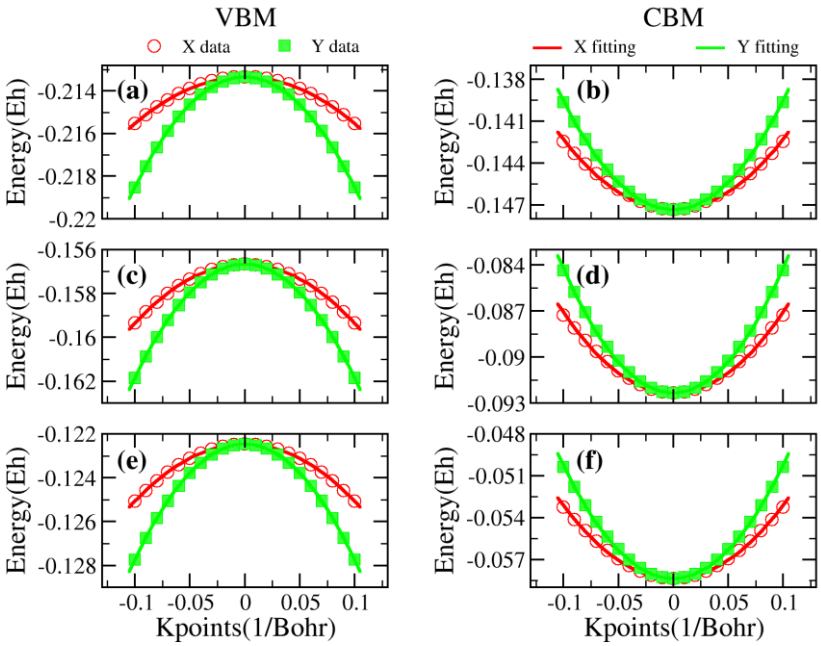

Fig. 4 The energy dispersion near the extreme points of the conduction band and valence band of the few layers of MoO3 calculated using the optB88-vdW functional.
Figures a and b, c and d, and e and f show the results of single-layer, double-layer and three-layer, respectively.

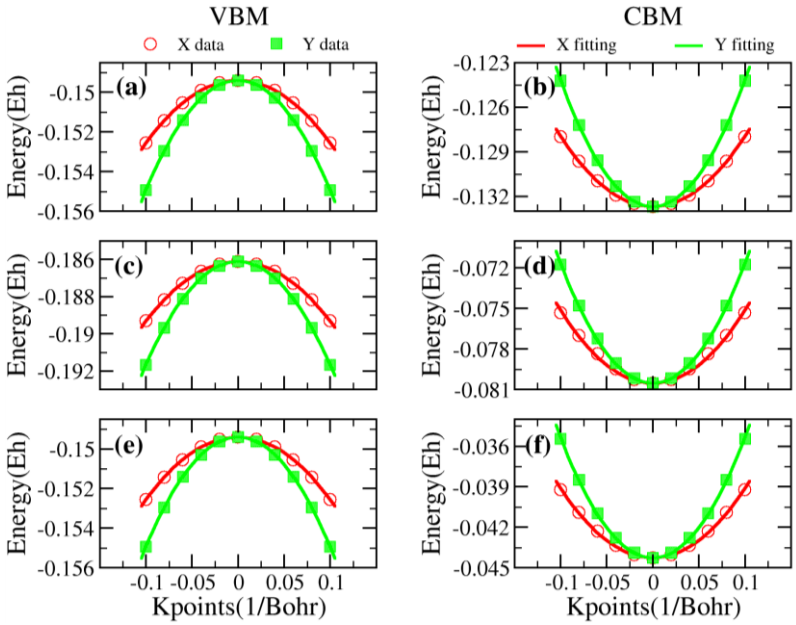

Fig. 5 The energy dispersion near the extreme points of the conduction band and valence band of the few layers of MoO3 calculated using the HSE06 functional.
Figures a and b, c and d, and e and f show the results of single-layer, double-layer and three-layer, respectively.

The deformation potential in the propagation direction of the longitudinal sound wave is another relevant factor that determines the mobility. The absolute band edge calculated by the optB88-vdW functional as a function of uniaxial strain is given in Figure 6, where the absolute band edge is defined as the difference between the vacuum electrostatic potential in VBM (CBM) and DFT. The HSE06 calculation gives similar results and trends, as shown in Figure 7. We found that when the uniaxial strain along the y direction, the VBM and CBM of the few layers of MoO3 reactively move to the high-energy region and the low-energy region. However, the x-direction uniaxial strain response to the absolute band edge is exactly the opposite. In addition, the slope of the y-axis curve is much larger than that of the x-axis, which indicates that the anisotropy of the deformation potential is larger. We

also found that the deformation potential of electrons is usually greater than that of holes. As shown in Table 1, the electronic deformation potentials of the single-layer MoO3 along the x-axis and y-axis given by the HSE06 functional are 2.220 and 11.443 eV, respectively, and the ratio reaches more than 5. For holes, the corresponding results are 1.999 and 9.538 eV. For graphene[15], the deformation potential on the x-axis is less than 5.0 eV, and the deformation potential of MoS2[14] is 3.9 -11 eV. Comparing the data, the PBE and optB88-vdW methods give smaller results than HSE06.

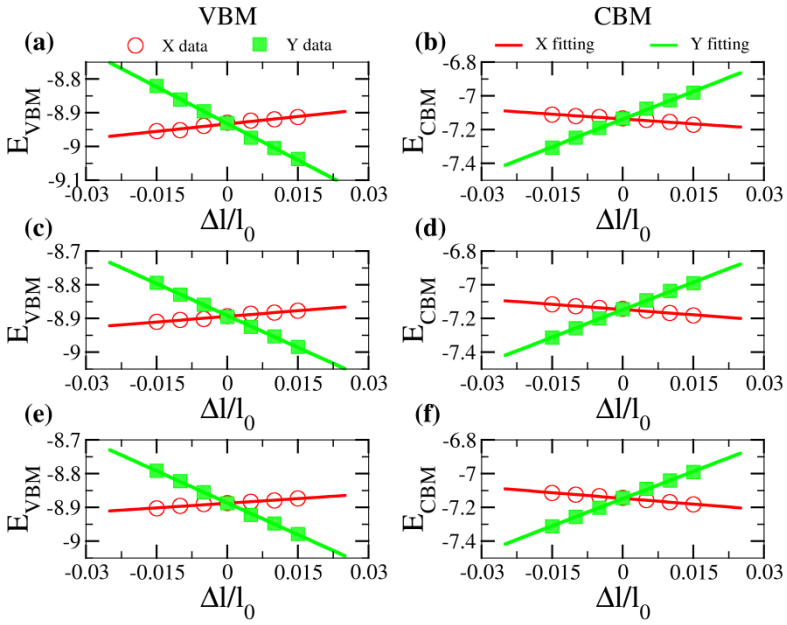

Fig. 6 The absolute band edge of the uniaxial strain along the x(a) and y(b) directions of the few-layer MoO3 calculated using the optB88-vdW functional. Figures a and b, c and d, and e and f show the VBM and CBM results of single-layer, double-layer and triple-layer MoO3, respectively.

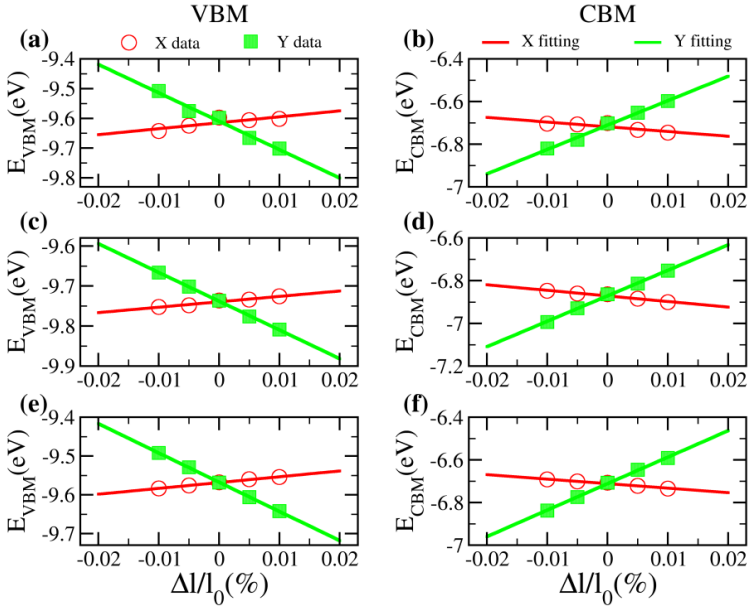

Fig. 7 The absolute band edge of the uniaxial strain of the few layers of MoO3 along the x(a) and y(b) directions calculated using the HSE06 functional.
Figures a and b, c and d, and e and f show the VBM and CBM results of single-layer, double-layer and triple-layer MoO3, respectively.

Based on the calculated effective carrier mass, elastic modulus and deformation potential, the carrier mobility of the few layers of MoO3 propagating in different directions is predicted. Generally compared with the optB88-vdW and PBE methods, the HSE06 functional gives a relatively small mobility due to the larger deformation potential. As shown in Table 1, we found that the electron and

hole mobility in the x direction is on the order of hundreds to thousands of square centimeters per volt per second, but only tens to hundreds on the y axis, it exhibits very large directional anisotropy, and the ratio is about 20-30 times larger. This high carrier mobility in the x-direction results from a very small deformation potential and a relatively large 2D elastic modulus. Compared with multi-layer black phosphorous, the deformation potential of MoO3 in the x-direction is usually 2-3 times smaller, and the corresponding 2D elastic modulus is 5-7 times larger. This means that the mobility of the few layers of MoO3 in the x direction is greater. In addition, the effective mass of the few layers of MoO3 seems to be 4-5 times greater than the effective mass of layered black phosphorus. According to Equation 1, the effective mass is inversely proportional to the mobility, resulting in a few layers of MoO3 with very high electron and hole mobility in the x direction, where the mobility of the three layers of MoO3 in the x direction is as high as 3000 cm2V-1s-1, This is comparable to the mobility of few layers of black phosphorus[4] and its 1D nanostructure. On the other hand, the carrier mobility in the y-axis is not too high. As shown in Table 1, this low mobility on the y-axis can be attributed to the larger deformation potential and the smaller elastic modulus. In summary, we predict that the few-layer MoO3 system has a very high carrier mobility in the x direction. Recently, a larger carrier mobility (> 1100cm2V-1s-1)[9] has been observed in MoO3 based FETs, which is consistent with our calculations. In addition, we predict that the mobility of both electrons and holes is very high, which indicates that the few layers of MoO3 should be a promising candidate material for efficient hole transport applications. In recent years, MoO3 as an efficient hole transport layer for organic light-emitting diodes and organic photovoltaics has been intensively studied, which also confirms our prediction. At the same time, the carrier mobility exhibits a very strong in-plane anisotropic behavior, so it is very important to improve the performance of the device by controlling the direction of carrier transfer. On the other hand, most experimental devices are based on MoO3-x, which is lower than the standard stoichiometry. Therefore, the influence of oxygen vacancies on the electron energy gap, mobility and carrier concentration should be further considered to facilitate understanding all physical properties of electronic equipment which based on MoO3.

4. Conclusion

In summary, we have estimated the acoustic phonon carrier mobility of few-layer MoO3 through first-principles calculations and deformation potential theory. Our results show that their carrier mobility is as high as 3000 cm2V-1s-1 at room temperature, and in addition, they exhibit strong anisotropic behavior. We also found that the direction-dependent larger elastic modulus and smaller deformation potential work together to promote the anisotropy of the high mobility transmission of the few layers of MoO3. This indicates that the few layers of MoO3 are a promising candidate material for electron and hole transport applications. In addition, we also suggest that by reasonably controlling the direction of carrier transfer, the performance of the device can be greatly promoted.

Acknowledgements

This work is supported by school-level scientific research project of Guangdong University of Science and Technology in 2020, project number: GKY-2020KYQNK-4.

References

[1] Novoselov K S, Geim A K, Morozov S V, et al. Electric field effect in atomically thin carbon films[J]. science, 2004, 306(5696): 666-669.

[2] Mak K F, Lee C, Hone J, et al. Atomically thin MoS2: a new direct-gap semiconductor[J]. Phys Rev Lett, 2010, 105(13): 136805.

[3] Wang Q H, Kalantar-Zadeh K, Kis A, et al. Electronics and optoelectronics of two-dimensional transition metal dichalcogenides[J]. Nat Nanotechnol, 2012, 7(11): 699-712.

[4] Qiao J, Kong X, Hu Z X, et al. High-mobility transport anisotropy and linear dichroism in few-layer black phosphorus[J]. Nat Commun, 2014, 5.

[5] Ji F, Ren X, Zheng X, et al. 2D α-MoO3 nanosheets for superior gas sensors[J]. Nanoscale, 2016, 8(16): 8696-8703.

[6] Saji V S, Lee C W. Molybdenum, molybdenum oxides, and their electrochemistry[J]. Chem Sus Chem, 2012, 5(7): 1146-1161.

[7] Brezesinski T, Wang J, Tolbert S H, et al. Ordered mesoporous α-MoO3 with iso-oriented nanocrystalline walls for thin-film pseudocapacitors[J]. Nat Mater, 2010, 9(2): 146-151.

[8] Huang L, Xu H, Zhang R, et al. Synthesis and characterization of gC3N4/MoO3 photocatalyst with improved visible-light photoactivity[J]. Appl Surf Sci, 2013, 283: 25-32.

[9] Balendhran S, Deng J, Ou J Z, et al. Enhanced charge carrier mobility in two-dimensional high dielectric molybdenum oxide[J]. Adv Mater, 2013, 25(1): 109-114.

[10] Alsaif M M Y A, Chrimes A F, Daeneke T, et al. High-Performance Field Effect Transistors Using Electronic Inks of 2D Molybdenum Oxide Nanoflakes[J]. Adv Funct Mater, 2016, 26(1): 91-100.

[11] Kaasbjerg K, Thygesen K S, Jacobsen K W. Phonon-limited mobility in n-type single-layer MoS2 from first principles[J]. Phys Rev B, 2012, 85(11): 115317.

[12] Bardeen J, Shockley W. Deformation potentials and mobilities in non-polar crystals[J]. Phys Rev Lett, 1950, 80(1): 72.

[13] Klimeš J, Bowler D R, Michaelides A. Van der waals density functionals appliedto solids[J], Phys Rev B, 2011, 83: 195131.

[14] Cai Y, Zhang G, Zhang Y W. Polarity-reversed robust carrier mobility in monolayer MoS2 nanoribbons[J]. J Am Chem Soc, 2014, 136(17): 6269-6275.

[15] Xi J, Long M, Tang L, et al. First-principles prediction of charge mobility in carbon and organic nanomaterials[J]. Nanoscale, 2012, 4(15): 4348-4369.